Fibers and Polymers 2006, Vol.7, No.4, 372-379

Green Composites. I. Physical Properties of Ramie Fibers for Environment-friendly Green Composites

Sunghyun Nam and Anil N. Netravali*

Fiber Science Program, Cornell University, Ithaca, NY 14853-4401, USA
(Received March 23, 2006; Revised September 28, 2006; Accepted December 4, 2006)

Abstract: The surface topography, tensile properties, and thermal properties of ramie fibers were investigated as reinforcement for fully biodegradable and environmental-friendly 'green' composites. SEM micrographs of a longitudinal and cross-sectional view of a single ramie fiber showed a fibrillar structure and rough surface with irregular cross-section, which is considered to provide good interfacial adhesion with polymer resin in composites. An average tensile strength, Young's modulus, and fracture strain of ramie fibers were measured to be 627 MPa, 31.8 GPa, and 2.7 %, respectively. The specific tensile properties of the ramie fiber calculated per unit density were found to be comparable to those of E-glass fibers. Ramie fibers exhibited good thermal stability after aging up to 160 °C with no decrease in tensile strength or Young's modulus. However, at temperatures higher than 160 °C the tensile strength decreased significantly and its fracture behavior was also affected. The moisture content of the ramie fiber was 9.9 %. These properties make ramie fibers suitable as reinforcement for 'green' composites. Also, the green composites can be fabricated at temperatures up to 160 °C without reducing the fiber properties.

Keywords: Ramie fiber, Green composite, Surface topography, Tensile properties, Thermal properties

Introduction

Natural plant-based cellulose fibers, particularly the ones that are long such as flax, jute, henequen, sisal, pineapple and ramie have gained attention as reinforcement for composites, because of their low cost, low density, high specific strength and modulus as well as good insulating and acoustic properties [1-9]. Several studies have reported on the excellent potential of using natural fibers in both thermoset and thermoplastic resins to form composites [3-13]. Also, these natural fibers are yearly renewable, i.e., fully sustainable, are biodegradable and available abundantly worldwide. In the development of composites, however, they exhibit certain drawbacks such as incompatibility with hydrophobic polymer resins. They also show poor resistance to moisture and swell as they absorb water [14].

The properties of natural plant fibers not only vary depending on origin, quality of the plant, location, weather, age, and preconditioning or processing but are also highly influenced by their chemical structure in terms of degree of polymerization (DP), cellulose content, orientation and crystallinity [13,15]. Compared to glass fibers, commonly used in composites, natural fibers have lower tensile strength. However, when the specific tensile strength (tensile strength/density) is considered, some natural fibers have comparable values to that of glass fibers because of their lower density. It has been reported that the ultimate microfibrils or nanofibrils of flax fibers have a Young's modulus almost as high as that of aramid fibers [16]. According to Cazaurang-Martinez *et al.* [2], henequen fibers could be used as a reinforcing agent for the preparation of composite materials based on their physical and mechanical properties. Luo and Netravali [6] studied the compatibility of henequen fibers with thermoplastic PHBV resin in terms of interfacial shear strength (IFSS) and also fabricated 'green' composites. Lodha and Netravali [7] characterized the properties of ramie fibers, and made fully biodegradable and environment-friendly 'green' composites with soy protein isolate polymer with good mechanical properties.

The thermal properties of fibers are very important since the fibers are likely to be exposed to high curing temperatures used during composite fabrication with thermoset resins or to high extrusion temperatures with thermoplastic resins. Since natural cellulose fibers are mixture of organic components, e.g., cellulose, hemicellulose, lignin, etc., thermal treatment leads to a variety of chemical and physical changes [14]. Heat has been shown to degrade hemicellulose and cellulose long before it degrades lignin [17]. Using thermogravimetric analysis (TGA), it was found that the natural fibers start to degrade between 220 and 280 °C, at which the degradation of hemicellulose occurs, and lignin degrades in the range of 280-300 °C [14]. The lignin, mostly hydrocarbon, contributes to char formation and insulates the fibers from further thermal degradation [18].

The thermal aging of natural fibers deteriorates their mechanical properties. Sridhar *et al.* [19] studied the thermal stability of jute fibers and found that tensile strength decreased by 60 % at 300 °C under vacuum for 2 hours due to the depolymerization of fibers. On the other hand, Gonzalez and Mayers [20] studied the thermal degradation of wood/polymer composites at temperatures ranging from 220 °C to 260 °C. Although the tensile strength and modulus deteriorated as a result of thermal degradation of wood flour, they found that

*Corresponding author: ann2@cornell.edu

the toughness and bending strength of the composites were more severely affected. Thermal degradation of fibers also produces volatiles at temperatures above 200 °C, which can lead to porous polymer products with lower densities and inferior mechanical properties [14].

All cellulose fibers are hydrophilic in nature, because the hydroxyl (-OH) groups on cellulose macromolecule are readily available for interaction with water molecules by hydrogen bonding not only at the surface but also in the bulk. The moisture content of cellulose fibers ranges from 8 % to 12.6 % depending on the crystalline content, void content and purity of the fiber [21]. For example, non-washed sisal fibers absorb water at least twice as much as washed fibers due to the presence of pectin [22]. In relation to the crystalline structure of cellulose, only a small amount of water can interact with the surface hydroxyl groups of the crystalline phase [23]. The hydrophilic nature of natural fibers lowers their compatibility with hydrophobic polymeric resins such as polyethylene and polypropylene [13]. During the processing of composites, the high moisture content of cellulose fibers can lead to poor processing abilities and products with high porosity [14]. Over long periods of time, the porosity can also influence resistance to weathering conditions in relation to relative humidity and dimensional stability, which finally affects the mechanical properties of the composites [23]. Moisture at the fiber/resin interface also reduces the interfacial bonding affecting the mechanical properties of the composites. Costa and D'Almedia [24] studied the water absorption of sisal and jute fiber-reinforced epoxy and polyester composites using the Fickian model of diffusion. The jute/epoxy composites showed the best mechanical properties and were the least affected by the exposure of the composites to distilled water due to the higher moisture resistance of jute fibers as well as good fiber/matrix interface. The physical and chemical modifications of natural fibers can reduce moisture affinity and improve the hydrophobicity of natural fibers [25-27].

Ramie fibers are readily available since they can be harvested three times per year with high production. Only the bast fiber in outer culm of the ramie plant can be used. Typically the length of a ramie fiber varies between 60 and 500 mm, and its diameter ranges from 20 to 35 μm. Ramie fiber is one of the strongest of all plant fibers to have high proportion of cellulose (65-75 %) and low proportion of lignin (1-2 %) in comparison with wood (40-50 % of cellulose and 15-35 % of lignin) [28]. When ramie fiber is peeled off from ramie culm, it is in the form of bundles of many individual ramie fibers bonded together. These bundles can be processed to separate to a required diameter, or can be used directly without separation to prevent fiber damage [29].

In this study, the physical properties of ramie fibers were investigated for use as reinforcement in the fabrication of 'green' composites. Surface topography, tensile, and thermal properties of ramie fibers were evaluated. The second part of this paper discusses the properties of green composites made using ramie fibers and soy protein concentrate based resin.

Experimental

Diameter Measurement

Ramie fibers were obtained in Seocheon-gun, Korea. The fiber specimens were between 600 and 1700 mm long. The diameter of ramie fibers was determined using a Leitz polarized light microscope (Ortholux model) with a calibrated eyepiece. Several precautions were taken to ensure accurate measurements of the fiber diameters, given their highly irregular cross-sectional shape. Five 1700 mm long fibers were selected to measure the variation in diameters along their lengths. Measurements were made at 100 mm intervals. Diameter at each point was calculated as an average value of two measurements, which were made by carefully rotating the fiber 90 ° about the longitudinal axis.

Thermal Treatment of Ramie Fibers

To investigate the effect of short term heating on the tensile properties of ramie fibers, individual single fiber specimens were heated at 100, 120, 140, 160 and 200 °C in an air-circulating oven for two time periods of 0.5 and 2 hours. These heating conditions were determined based on the hot pressing or resin curing times and temperatures commonly used during composite fabrication. Following the heat treatment, specimens were conditioned at 21 °C and 65 % relative humidity (RH) for 24 hours prior to characterizing their properties.

Tensile Properties

The tensile properties, including tensile strength, Young's modulus, fracture strain and energy to break of ramie fibers were measured according to ASTM D 3379-89 using an Instron tensile testing machine, model 1122. All tests were performed under standard ASTM conditions of 21 °C and 65 % RH. The diameter of single fibers was measured using a Leitz polarized light microscope. Individual single fiber specimens were mounted and glued on a paper tab using Super Glue® [7]. The average diameter value was calculated from five measurements made at different locations along the length of each fiber. The gauge length was kept at 50 mm, and the testing was performed at a crosshead speed of 20 mm/min, or a strain rate of 0.4 min^{-1} so as to obtain the fracture within one minute. Fifty single fiber specimens were picked out randomly and measurements were made. The tensile strength data were fitted to a 2-parameter Weibull distribution [30,31]. Most high strength and brittle fibers including graphite and Kevlar® show excellent fit to the Weibull distribution. For the effects of heating on the tensile properties of ramie fibers, ten successful tests were conducted to obtain an average value.

Surface Characterization

Both longitudinal and cross sectional views of ramie fibers

were characterized using a scanning electron microscope (SEM), Leica model 440X. Excitation energy values of 5 and 25 keV were used with a beam current of 0.5 nA. All specimens were sputtered with gold before examination in order to ensure good conductivity. To obtain cross-sectional view, the fiber was embedded in epoxy resin, and sectioned using a microtome.

Moisture Content

The moisture content of the ramie fibers was measured using a Brabender moisture/volatile tester at 130 °C according to ASTM D 2654-89a. The moisture content value was obtained from the level-off point in weight loss versus drying time plot. Three separate measurements were used to obtain the average value of the moisture content.

Results and Discussion

Surface Topography and Diameter

Figure 1 shows typical longitudinal views of ramie fibers. The fibrillar separation and rough surface, arising from the fibrillar nature of the ramie fibers, can be seen in Figures 1(a) and (b), respectively. It is seen that the fibrils are not bonded strongly with each other and can be easily separated. However, this is believed to be the effect of the fiber processing, where the bundles of ramie fibers are peeled off from ramie culm. This separation may be performed by hand or machine to have a proper diameter for the desired application. Also various chemical treatments such as NaOH and higher temperatures are commonly used to remove a hard outer shell as well as hemicellulose and lignin. Some harsh mechanical or chemical processing allows easy separation of fibrils, whereas fibers processed in a mild manner might not see easy separation of the fibrils. Figure 2 shows a cross-sectional view taken from the middle part of a single fiber. The cross-section is not round but irregularly elliptical. The inter-fibrillar separation, which was observed in the longitudinal view, can be seen clearly in the cross-sectional view. The irregular cross-section and fibrillar structure could lead to a higher estimate of the diameter, which results in wider strength variation as well as lower strength values. Nam and Netravali [32] showed that this surface roughness of ramie fibers contributed to high interfacial shear strength with soy protein concentrate (SPC) polymer resin by increasing the mechanical interlocking and

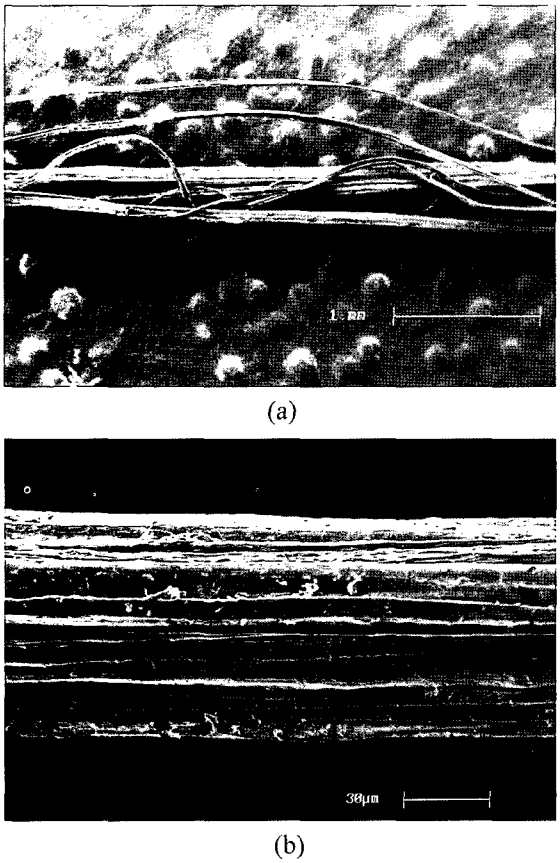

(a)

(b)

Figure 1. Typical SEM photomicrographs of longitudinal views of ramie fibers; (a) fibrillar separation and (b) surface roughness.

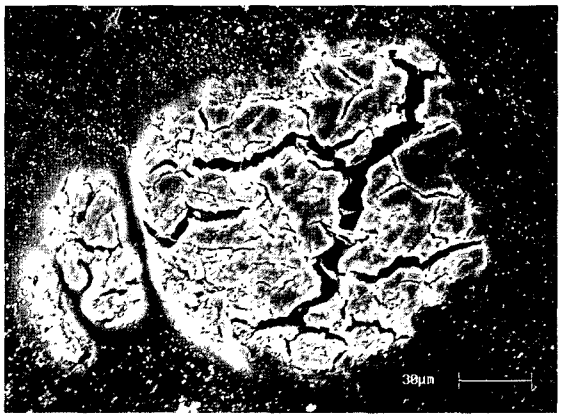

Figure 2. Typical SEM micrograph of a cross-sectional view of a single ramie fiber.

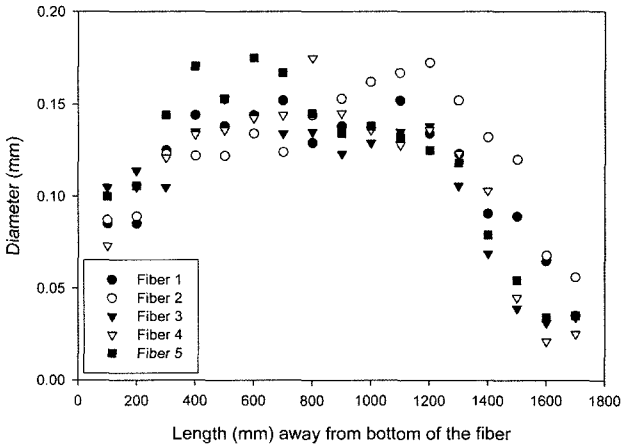

Figure 3. Diameters of ramie fibers along the length.

interfacial area. Also, the tube-like cellular structure of the ramie fibers is expected to provide good thermal and sound insulation properties.

The distribution of fiber diameters along fiber length was investigated using the optical microscope method. The diameters of single fibers were measured from the bottom part to the tip of the fiber and are presented in Figure 3. Compared with the middle section of the fiber, the bottom and the end parts have smaller diameter. Note also that the diameters of the middle part remain relatively constant over about 800 mm of the fiber length. Although the diameters at the tip may be expected to be smaller, lower diameters at the bottom may be an artifact created by the fiber processing. The average diameter of the ramie fibers was calculated to be 0.12 mm with a standard deviation of 0.04 mm. In contrast to melt spun synthetic fibers emerging from a spinneret which have uniform diameters and a specific cross-sectional shapes, ramie fibers, like other natural plant-based fibers, exhibit wide variability in diameter and irregular cross-sectional shape. As a result of this variation, it is difficult to calculate precise diameter or perimeter of these fibers.

Tensile Properties

Table 1 presents the tensile properties of ramie fibers including tensile strength, Young's modulus, fracture strain and energy to break. It can be seen that ramie fibers have a large amount of variability in their tensile properties. This may be attributed to the inherent irregularity of the natural fibers and various defects and is commonly seen in most natural fibers. Barkakaty [33] has reported that the tensile properties of natural fibers depend on the microfibrillar orientation in the secondary wall of the plant cell. The difference in this angular orientation along the fiber with respect to the direction of the applied load could cause the variations in tensile properties. Lodha and Netravali [7] obtained ramie fibers from Danforth International Trade Associates Inc., New Jersey, and measured their tensile properties at a gauge length of 50 mm and a strain rate of 0.2 min^{-1}. Their results showed that the ramie fiber had an average tensile strength of 661.2 MPa, fracture strain of 1.9 %, Young's modulus of 67.9 GPa, and energy to break of 7.2 J. Other studies have reported the tensile strength of ramie fibers between 400 and 938 MPa [21,34]. The fibers show a brittle fracture which is consistent with other researchers [7,21,34]. However, different fibrils fractured at different locations in the case of control fibers.

These tensile properties of ramie fibers were compared with

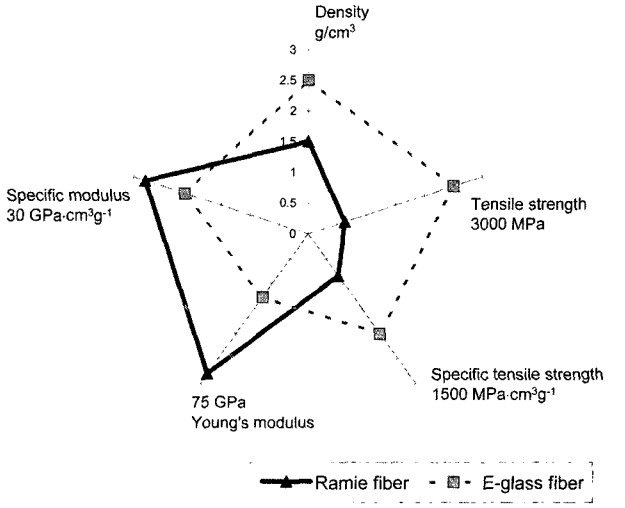

Figure 4. Comparative tensile properties of ramie and E-glass fibers.

those of E-glass fibers obtained from other literature [21] and presented in Figure 4. It can be seen that E-glass fibers have higher average tensile properties than ramie fibers. However, the specific tensile properties of ramie fiber, calculated per unit density, fall within the same range as those of E-glass fibers. While the specific tensile strength of E-glass fibers are higher than ramie fibers, specific modulus of ramie fibers is significantly higher than E-glass fibers. These favorable tensile properties coupled with the low density of the ramie fibers indicate that they can be effectively utilized as a reinforcing component in composite applications where weight reduction is critical.

The tensile strength data of ramie fiber were fitted to a two-parameter Weibull distribution of the form shown in equation (1) [30]:

$$W(X) = 1 - \exp\left[-\left(\frac{X}{X_o}\right)\right]^R \quad (1)$$

where X is the tensile strength of the fiber, $W(X)$ is the probability that the tensile strength of the fiber is less than X, X_o is the scale parameter, and R is the shape parameter. The Weibull scale parameter represents 63rd percentile of tensile strength and the shape parameter shows the variability of tensile strength. The Weibull plot is presented in Figure 5. It is seen that the Weibull probability distribution provides a good fit for the experimental tensile strength data of ramie

Table 1. Tensile properties of ramie fibers*

Density (g/cm^3)	Tensile strength (MPa)	Specific stress ($MPa \cdot cm^3/g$)	Fracture strain (%)	Young's modulus (GPa)	Energy to break (J)
1.5**	627 (25.8)***	418	2.7 (14.4)	31.8 (33.7)	7.8 (35.8)

*The strain rate of 0.4 min^{-1} was used, **the number was obtained from the Handbook of Fiber Chemistry [35], ***numbers in parentheses show the percent coefficient of variation for each measurement.

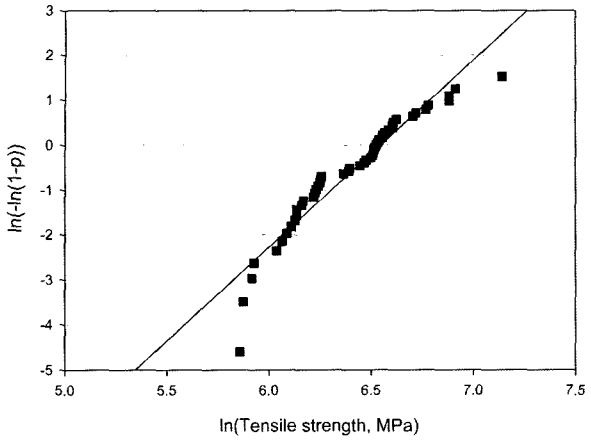

Figure 5. Weibull plot for ramie fiber tensile strength.

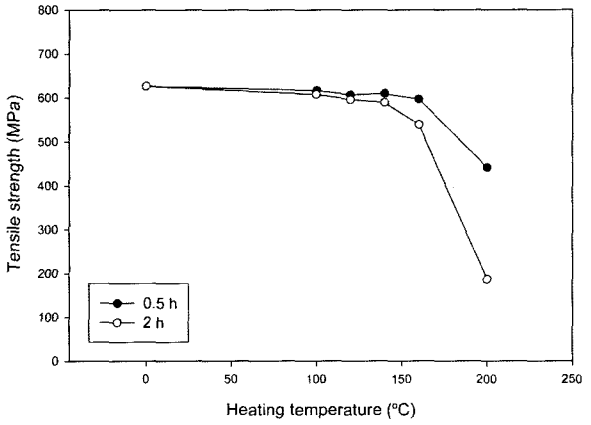

Figure 6. Effect of thermal treatments on the tensile strength of ramie fibers.

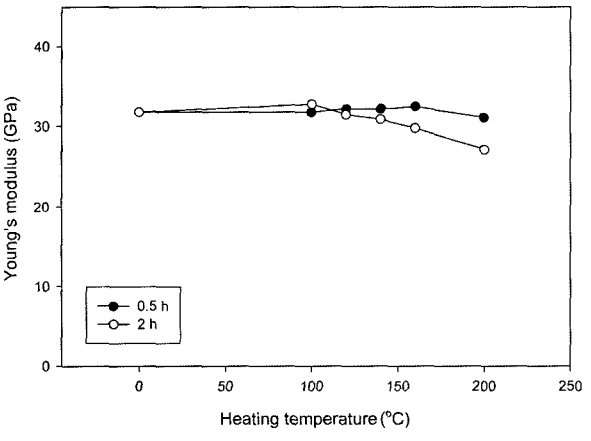

Figure 7. Effect of thermal treatments on the Young's modulus of ramie fibers.

fibers, except for the upper and lower tails. The Weibull scale and shape parameters of ramie fiber tensile strength were calculated to be 696.3 MPa and 4.16, respectively.

Table 2. Scale and shape parameters of untreated and heat-treated ramie fiber strength distribution

Treatment temperature/time	Scale parameter (MPa)	Shape parameter
Control (untreated)	696.3	4.16
100 °C/0.5 h	711.7	5.83
100 °C/2 h	642.6	5.03
120 °C/0.5 h	639.1	5.23
120 °C/2 h	649.8	4.90
140 °C/0.5 h	656.5	4.31
140 °C/2 h	594.7	6.19
160 °C/0.5 h	667.9	4.37
160 °C/2 h	574.5	7.63
200 °C/0.5 h	459.7	7.40
200 °C/2 h	200.5	6.80

Thermal Properties

Changes in mechanical properties of ramie fibers were investigated after heat treatment (thermal aging) at various temperatures in an air-circulating oven for 0.5 hours and 2 hours. Figures 6 and 7 show the effect of heating temperature and time on the tensile strength and Young's modulus of ramie fibers, respectively. Table 2 presents Weibull scale and shape parameters for untreated (control) and heat-treated ramie fibers. All fibers after heat treatment also retained their brittle fracture nature.

Up to a heating temperature of 160 °C, no statistical difference in the tensile strength was observed, regardless of the heating time ($p \geq 0.05$), up to 2 hours. In the case of Young's modulus, there were no significant differences between unheated and heated ramie fibers ($p \geq 0.05$). However, the modulus dropped at 200 °C. Saheb and Jog [14] explained that the thermal stability of plant-based natural fibers is because of the cell walls that undergo pyrolysis. With increasing temperature, the outer layers contribute to char formation on the cell walls. Once formed, the charred layers insulate the inner fiber from further thermal degradation. With further increase in the heating temperature to 200 °C, however, tensile strength decreased significantly by 30 % after 0.5 hours and by 70 % after 2 hours ($p \leq 0.05$). A similar phenomenon was also observed by Ochi *et al.* [36]. They found that the tensile strength of bamboo and Manila hemp fibers decreased after 1 hour at 160 °C and at 180 °C, respectively. As reported by Bledzki *et al.* [37], no thermal degradation takes place until 160 °C. At temperatures above 200 °C, however, thermal degradation leads to a considerable weight loss of up to 30 % due to depolymerization and oxidation. Saheb and Jog [14] explained the thermal degradation of cellulose fibers as a two-stage process. The first stage occurs in the temperature range of 220-280 °C when hemicellulose and cellulose degrade and the second in the range of 280-300 °C when the lignin starts to degrade. The activation energies for the two

processes are about 28 and 35 kcal/mol, which correspond to the degradation of hemicellulose/cellulose and lignin, respectively. Since our study was limited to aging at 200 °C, only hemicellulose/cellulose present in the outside layers was expected to be affected. Based on the trend observed in degradation of tensile strength and Young's modulus induced by temperature exposure, it can be inferred that thermal treatments at and above 200 °C reduce the fiber tensile strength significantly. This clearly indicates that the processing temperatures for ramie fibers need to be held below 200 °C to limit the losses in their mechanical properties. It is also seen from Table 2 that shape parameters increased for all heat-treated fibers, indicating that the variation in the properties decreased after the heat treatment. This may be related to the change in fracture behavior as a result of heat aging. While the fracture of untreated fibers is initiated through weaker individual fibrils fracturing at different locations along the fiber length and separating from the fiber, the heat-treated (aged) fibers fractured in a brittle manner and the fibrils remained bound. However, all fibers, control or treated, showed brittle fracture. In other words, fibers did not show any yielding behavior. These different fracture behaviors are discussed in SEM micrographs of the fracture surfaces.

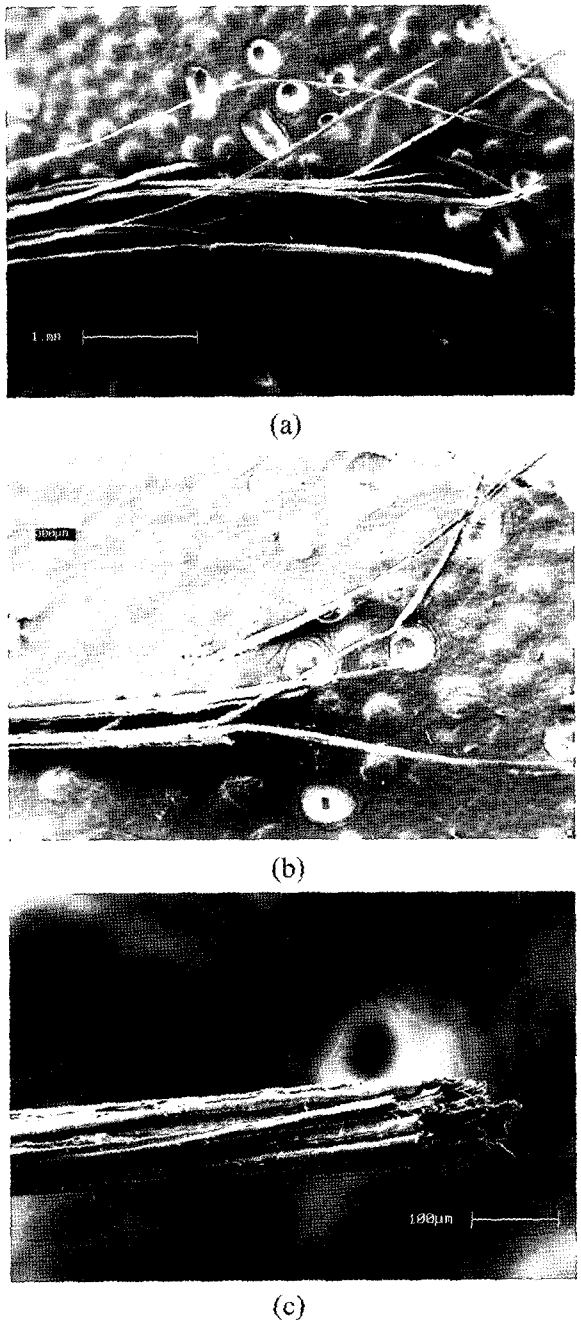

(a)

(b)

(c)

Figure 8. SEM photomicrographs of tensile fractured ramie fibers; a) unheated (control), (b) heat-treated at 120 °C for 2 h, and (c) eat-treated at 200 °C for 2 h.

Figure 8 shows the SEM micrographs of the fracture surfaces of control and heat treated ramie fibers after tensile tests. The fracture surface of fiber heated at 140 °C for 2 hours (Figure 8b), which is a procedure similar to the curing process for composites, was compared with that of control (unheated) fiber (Figure 8a). In order to investigate the effect of high thermal treatment on the fracture behavior of fibers, the fracture surface of fiber heated at 200 °C for 2 hours (Figure 8c) was also observed. The fracture surface of control fiber shows that the individual fibrils fracture at different locations. Although the fracture was brittle, the fracture is spread over a large length as a result of fibril fractures. Fiber treated at 120 °C for 2 hours also shows similar separation of fibrils. These similar fracture behaviors indicated that heat treatment at 120 °C for 2 hours did not affect the fiber properties significantly. This also confirms the tensile results that showed no change in their tensile properties. However, the fiber heated at 200 °C for 2 hours fractured without fibril splitting, consistently resulting in a clean and transverse fracture surface with almost no fibrillation. As mentioned earlier, it has been shown that lignin takes much longer to degrade by heat than cellulose and hemicellulose [18]. Therefore, even though cellulose and hemicellulose may have degraded by the thermal treatment, the lignin component binding the fibrils may still exist in undegraded form. It has been reported that the temperature range of 280-300 °C is associated with the degradation of lignin [14]. On the other hand, crystalline cellulose, which is less resistant to heat, weakened the strength of the fibers, as was observed in Figure 6. This type of fracture of the fibers with no fibril separation may absorb less energy and thus reduce the toughness of the composites.

Moisture Content

A typical weight loss vs. drying time curve at 130 °C is presented in Figure 9. It can be seen that the ramie fibers lost moisture rapidly and reached equilibrium weight in the first 10 minutes. The moisture content of the ramie fiber was 9.9 %, which is in the reported moisture content range from 8 % to 12.6 % of the natural fibers. Like all other cellulose

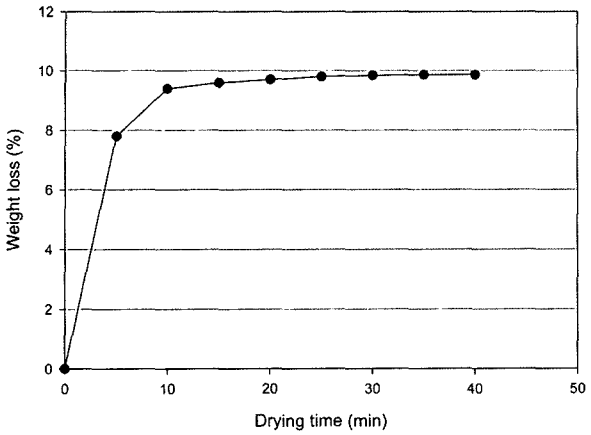

Figure 9. Weight loss versus drying time for ramie fibers at 130 °C.

fibers ramie fiber exhibits a hydrophilic nature due to their hydroxyl (-OH) groups. This high moisture content of ramie fibers could lead to dimensional instability in composites and also affect the fiber/resin interface resulting in lowering of the composite mechanical properties. These results indicate that if these fibers are to be used with hydrophobic resin composites, fiber preparation should include complete drying to avoid the problems associated with the moisture present in the fiber.

Conclusion

In the present research, the tensile and thermal properties of ramie fibers were studied as reinforcement of environment-friendly biodegradable composites. Following conclusions were drawn:

1) Ramie fibers were found to have a variable diameter along their length with an average diameter of 0.123 mm. SEM micrographs revealed that ramie fibers have a fibrillar structure and irregular cross-section.

2) Ramie fibers had an average tensile strength of 627 MPa, Young's modulus of 31.8 GPa and fracture strain of 2.7 %. High specific tensile properties calculated per unit density of these fibers are considered to be good for consideration as reinforcing element in composites.

3) The heat treatment did not influence the tensile strength and modulus of ramie fibers up to 160 °C and ramie fiber showed hydrophilic nature. At temperature of 200 °C, however, the fibers lost their strength significantly after 2 hours of heat treatment.

References

1. E. E. Sera, L. Robles-Austriaco, and R. P. Pama, *J. Ferrocement*, **20**, 109 (1990).
2. M. N. Cazaurang-Martinez, P. J. Herrera-Franco, P. I. Gonzalez-Chi, and M. Aguilar-Vega, *J. Appl. Polym. Sci.*, **43**, 749 (1991).
3. K. Joseph, S. Thomas, C. Pavithran, and M. Brahmakumar, *J. Appl. Polym. Sci.*, **47**, 1731 (1993).
4. S. Luo and A. N. Netravali, *J. Mater. Sci.*, **34**, 3709 (1999).
5. S. Luo and A. N. Netravali, *Polym. Composite.*, **20**, 367 (1999).
6. S. Luo and A. N. Netravali, *J. Adhes. Sci. Technol.*, **15**, 423 (2001).
7. P. Lodha and A. N. Netravali, *J. Mater. Sci.*, **37**, 3657 (2002).
8. P. Lodha and A. N. Netravali, *Polym. Compos.*, **26**, 647 (2005).
9. P. Lodha and A. N. Netravali, *Composites Science and Technology*, **65**, 1211 (2005).
10. B. V. Kokta, R. Chen, C. Daneault, and J. L. Valade, *Polym. Compos.*, **4**, 229 (1983).
11. C. Pavithran, P. S. Mukjerjee, M. Brahmakumar, and A. D. Damodaran, *J. Mater. Sci.*, **26**, 455 (1991).
12. M. Wollerdorfer and H. Bader, *Industrial Crops and Products*, **8**, 105 (1998).
13. A. K. Mohanty and M. Misra, *Polym-Plast. Technol. Eng.*, **34**, 729 (1995).
14. D. N. Saheb and J. P. Jog, *Adv. Polym. Tech.*, **18**, 351 (1999).
15. J. George, M. S. Sreekala, and S. Thomas, *Polym. Eng. Sci.*, **41**, 1471 (2001).
16. R. T. Woodhams, G. Thomas, and D. K. Rodgers, *Polym. Eng. Sci.*, **24**, 1166 (1984).
17. F. Shafizadeh, "The Chemistry of Solid Wood" (R. M. Rowell ed.), pp.489-529, American Chemical Society, Washington, 1984.
18. A. K. Mohanty, M. Misra, and G. Hinrichsen, *Macromol. Mater. Eng.*, **276**, 1 (2000).
19. M. K. Sridhar, G. Basavarajjappa, S. S. Kasturi, and N. Balsubramanian, *Indian J. Text. Res.*, **7**, 87 (1982).
20. C. Gonzalez and G. E. Mayers, *Int. J. Polym. Mater.*, **23**, 67 (1993).
21. A. K. Bledzki, S. Reihmane, and J. Gassan, *J. Appl. Polym. Sci.*, **59**, 1329 (1996).
22. T. T. Le Thi, H. Gauthier, R. Gauthier, B. Chabert, J. Guillet, B. V. Luong, and V. T. Nguygen, *J. Macromol. Sci. Pure Appl. Chem.*, **33**, 1997 (1996).
23. R. Gauthier, C. Joly, A. C. Coupas, H. Gauthier, and M. Escoubes, *Polym. Compos.*, **19**, 287 (1998).
24. F. H. M. M. Costa and J. R. M. D'Almedia, *Polym-Plast. Technol. Eng.*, **38**, 1081 (1999).
25. F. R. Al-Siddique, A. U. Khan, and R. A. Sheikh, *World Textile Abstr.*, **No. 4196**, (1984).
26. E. T. N. Bisanda and M. P. Ansell, *J. Mater. Sci.*, **27**, 1690 (1992).
27. A. Bismarck, A. K. Mohanty, I. Aranberri-Askargorta, S. Czapla, M. Misra, G. Hinrichsen, and J. Springer, *Green Chemistry*, **3**, 100 (2001).

28. D. Fengel and X. Shao, *Wood Sci. and Technol.*, **18**, 103 (1984).
29. S. Li, B. Zhou, Q. Zeng, and X. Bao, *Composites*, **25**, 225 (1994).
30. W. Weibull, *Ing. Vetenskaps. Akad. Handl.*, **151**, 153 (1939).
31. H. F. Wu and A. N. Netravali, *J. Mater. Sci.*, **27**, 3318 (1992).
32. S. Nam and A. N. Netravali, *J. Adhes. Sci. Technol.*, **18**, 1063 (2004).
33. B. C. Barkakaty, *J. Appl. Polym. Sci.*, **20**, 2921 (1971).
34. A. K. Bledzki and J. Gassan, *J. Prog. Polym. Sci.*, **24**, 221 (1999).
35. M. Lewin and E. M. Pearce Eds., "Handbook of Fiber Chemistry", Marcel Dekker, New York, 1998.
36. S. Ochi, H. Takagi, R. Takura, and R. Niki, *Jsms. Composites*, **30**, 131 (2001).
37. A. K. Bledzki, S. Reihmane, and J. Gassan, "Handbook of Engineering Polymeric Materials" (N. P. Cheremisinoff ed.), pp.787-810, Marcel Dekker, New York, 1998.